UNIVERSITY
OF WOLLONGONG
AUSTRALIA

University of Wollongong
Research Online

Faculty of Engineering and Information Sciences - Papers: Part A

Faculty of Engineering and Information Sciences

2013

Effect of austenitising and deformation temperatures on dynamic recrystallisation in Nb-Ti microalloyed steel

Andrii G. Kostryzhev
University of Wollongong, andrii@uow.edu.au

Abdullah Al Shahrani
University of Wollongong, amfa065@uowmail.edu.au

Chen Zhu
University of Sydney, czhu@uow.edu.au

Simon P. Ringer
University Of Sydney

Elena V. Pereloma
University of Wollongong, elenap@uow.edu.au

Publication Details

Kostryzhev, A. G., Al Shahrani, A., Zhu, C., Ringer, S. P. & Pereloma, E. V. (2013). Effect of austenitising and deformation temperatures on dynamic recrystallisation in Nb-Ti microalloyed steel. Materials Science Forum, 753 431-434.

Research Online is the open access institutional repository for the University of Wollongong. For further information contact the UOW Library: research-pubs@uow.edu.au

Effect of austenitising and deformation temperatures on dynamic recrystallisation in Nb-Ti microalloyed steel

Abstract

An investigation into influence of the austenitising temperature and the austenite deformation temperature on Nb precipitation and recrystallisation kinetics was carried out for a steel containing 0.081C-0.021Ti-0.064Nb (wt. %). The austenite grain structure was correlated to the dispersive properties of Nb atom clustering and precipitation. Irrespective of the austenitising temperature, deformation to 0.75 strain at 1075 °C produced a fully recrystallised microstructure. After deformation at 975 °C, only partial recrystallisation was observed in the samples austenitised at higher temperature, whereas samples austenitised at lower temperature were fully recrystallised. The influence of solute drag and particle pinning effects on the recrystallisation rate is discussed. © (2013) Trans Tech Publications, Switzerland.

Keywords

effect, ti, nb, recrystallisation, steel, dynamic, microalloyed, temperatures, deformation, austenitising

Disciplines

Engineering | Science and Technology Studies

Publication Details

Kostryzhev, A. G., Al Shahrani, A., Zhu, C., Ringer, S. P. & Pereloma, E. V. (2013). Effect of austenitising and deformation temperatures on dynamic recrystallisation in Nb-Ti microalloyed steel. Materials Science Forum, 753 431-434.

This journal article is available at Research Online: http://ro.uow.edu.au/eispapers/1273

Effect of austenitising and deformation temperatures on dynamic recrystallisation in Nb-Ti microalloyed steel

Andrii G. Kostryzhev[1a], Abdullah Al Shahrani[1], Chen Zhu[2], Simon P. Ringer[2] and Elena V. Pereloma[1]

1 – School of Mechanical, Materials and Mechatronic Engineering, Faculty of Engineering, University of Wollongong, NSW 2500, Australia

2 - Australian Centre for Microscopy and Microanalysis, and School of Aerospace, Mechanical and Mechatronic Engineering, The University of Sydney, NSW 2006, Australia

[a] e-mail: kostryzhev@yahoo.com

Key words: thermo-mechanical processing, precipitation, recrystallisation, microalloyed steel

Abstract. An investigation into influence of the austenitising temperature and the austenite deformation temperature on Nb precipitation and recrystallisation kinetics was carried out for a steel containing 0.081C–0.021Ti–0.064Nb (wt. %). The austenite grain structure was correlated to the dispersive properties of Nb atom clustering and precipitation. Irrespective of the austenitising temperature, deformation to 0.75 strain at 1075 °C produced a fully recrystallised microstructure. After deformation at 975 °C, only partial recrystallisation was observed in the samples austenitised at higher temperature, whereas samples austenitised at lower temperature were fully recrystallised. The influence of solute drag and particle pinning effects on the recrystallisation rate is discussed.

Introduction

The Nb solute atoms and precipitates pin the austenite grain boundaries and reduce the recrystallisation and grain growth rates, which leads to grain refinement and improved mechanical properties. An increase in Nb content in steel composition retards recrystallisation (the recrystallisation stop temperature, T_{nr}, increases [1]). Nb(C,N) precipitates were shown to pin the grain boundaries stronger than Nb solute atoms [2 - 4]. However, the Nb solute drag effect has a significant influence on recrystallisation at high temperatures, low strain levels, short interpass time and high cooling rate [5, 6], i.e. when the particle number density is low. Although a significant research was carried out to assess a dependence of the Nb precipitation kinetics (and related to it the pinning effect strength) on steel composition [1, 7 - 9] and strain levels [10 - 12], no final conclusion was made regarding the optimum precipitation parameters to maximise the grain boundary pinning effect. In the present paper a dependence of the austenite recrystallisation kinetics on the Nb precipitation kinetics was studied for the Nb-Ti-microalloyed steel.

Material and experimental techniques

The Nb-Ti-microalloyed steel of composition 0.081C, 1.20Mn, 0.27Si, 0.021Ni, 0.019Cr, 0.1Mo, 0.016Cu, 0.037Al, 0.064Nb, 0.021Ti, 0.003V, 0.001S, 0.012P, and 0.0047N (all in wt %) has been received from BlueScope Steel Ltd. For thermo–mechanical processing (TMP) simulations, samples of 10x15x20 mm size were cut from a quarter thickness position of a 230 mm thick continuously cast slab. The TMP was performed using Gleeble 3500 thermo-mechanical simulator (Fig. 1, a). To modify the Nb precipitate size distributions, the steel samples were heated to two temperatures (near the particle dissolution temperature and above it) and deformed at two temperatures (near T_{nr} and above it). All the samples were water quenched immediately after the finishing deformation in order to prevent Nb diffusion. This allowed studying the Nb clusters and precipitates in austenite. The prior austenite grain boundaries were revealed by etching for 5 min at 68 °C in a special reagent (aqueous picric acid + hydrochloric acid + detergent). To obtain the austenite grain size (equivalent circle diameter) distributions, 800-1000 grains were imaged using Leica DMRM optical microscope. For determination of the Nb-Ti-rich particle size distributions and the particle number density values, 2306 particles from all the four TMP conditions were imaged using JEOL 7001F FEG scanning electron microscope (SEM). Compositions of 57 particles from all the four TMP conditions were analyzed using energy dispersive X-ray spectroscopy (EDXS). The Nb atom cluster and Nb-C cluster size and number density for all the four TMP conditions were studied using atom probe tomography (APT). The APT data was collected on a Cameca® Local Electrode Atom Probe (LEAP), operating at a temperature of 20 K and a pulse fraction rate of 20% [13]. The APT specimen preparation included two stages of electropolishing using a solution of 25% perchloric + 75% glacial acetic acid during rough polishing, and a solution of 2% perchloric acid + 98% butoxyethanol during fine polishing [14].

Results and Discussion

Analysis of the stress-strain behaviour during finishing deformation (Fig. 1, b) has shown continues work-hardening for the "1250 °C reheating + 975 °C deformation" TMP schedule, which corresponds to incomplete recrystallisation observed on optical micrographs (Fig. 1, c). However, the other three schedules have shown the gradual decrease in stress after reaching a maximum, which corresponds to the optically observed equaxed grain structures (Fig. 1, d, e, f) and is an indicative of the dynamic recrystallisation. Such a variation in recrystallisation kinetics and stress-strain behaviour might be related to a variation in the Nb precipitation kinetics with the TMP schedule.

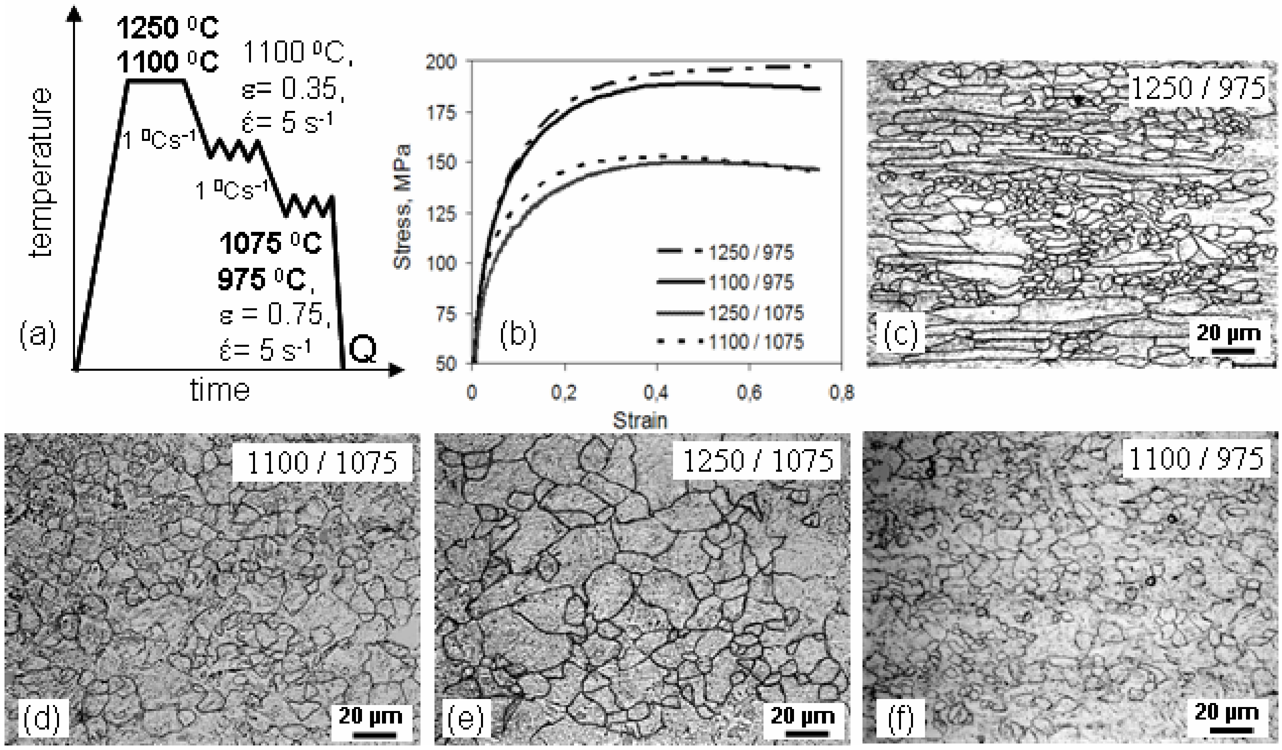

Fig.1 (a) TMP schedule scheme, (b) stress-strain curves during finishing deformation and (c,d,e,f) prior austenite microstructures for the four TMP schedules

The SEM imaging revealed presence of 20 – 130 nm precipitates for all the four TMP schedules (Fig. 2, Table 1). Two groups of precipitates have been separated by EDXS: (i) > 70 nm size ellipsoidal and cuboidal, mainly TiNb-rich; and (ii) < 70 nm size close to spherical shape, mainly Nb-rich particles. The parameters for > 70 nm particles did not show a significant variation with the TMP schedule (Table 1), which can be explained by the higher dissolution temperature / time of the particle Ti core compared to the austenitising temperature / time. However, within the < 70 nm size range with a decrease in austenitising temperature the average particle diameter decreased, the number density increased and the relative amount of the Nb-rich particles (to the total amount analysed) increased. These can be explained by the incomplete dissolution of Nb-rich particles during holding at 1100°C. With a decrease in deformation temperature both the particle number density within the < 70 nm size range and the relative amount of Nb-rich particles (to the total amount analysed) have increased. This can be explained by the longer time for precipitation (cooling time between the roughing and finishing deformations).

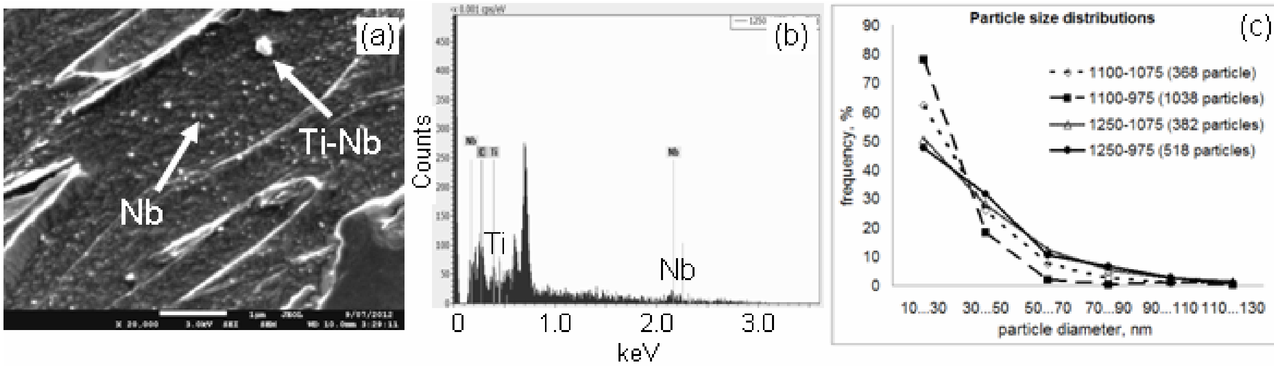

Fig. 2 Typical (a) SEM image of precipitates for "1100 °C reheating + 1075 °C deformation" TMP schedule and (b) EDS spectra of a TiNb-rich particle; (c)- particle size distributions

Table 1 Summary of the parameters for TiNb- and Nb-rich precipitates

Re-heating temperature [°C]		1100				1250			
Deformation temperature [°C]		1075		975		1075		975	
Particle size range [nm]		< 70	>70	< 70	>70	< 70	>70	< 70	>70
Number density [μm^{-2}]		3.13	0.13	12.06	0.21	2.05	0.21	2.75	0.31
Average diameter [nm]		26	96	22	107	29	92	29	84
Chemistry [%]	Nb	57	0	80	0	30	40	50	20
	Nb-Ti	43	100	20	100	70	60	50	80

The APT study of atom clusters has shown presence of C clusters, Nb clusters and Nb-C clusters of varying composition (Fig. 3) for all the four TMP conditions. With a decrease in austenitising temperature, the Nb content in the austenite matrix, the Nb cluster size and number density and the Nb-C cluster number density all decreased, although the Nb-rich particle number density increased (Table 2). These can be related to the incomplete dissolution of Nb-rich particles during holding at 1100°C. The number densities of Nb clusters, Nb-C clusters and Nb-rich particles all increased with a decrease in deformation temperature, which can be related to an increase in the time available for precipitation.

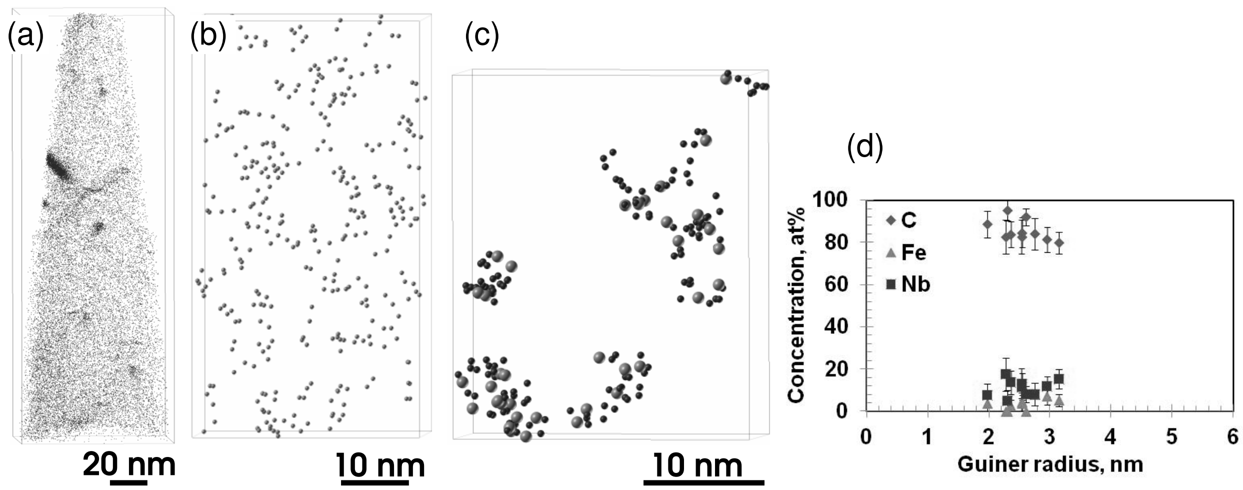

Fig. 3 (a) Carbon atom map and selected atom maps showing (b) Nb clusters and (c) Nb-C clusters (Nb - large and C - small spheres); (d) dependence of Nb-C cluster composition on cluster size (all for "1100 °C reheating + 1075 °C deformation" TMP schedule)

Partial recrystallisation of the austenite grain structure was observed for the TMP condition (1250°C reheating + 975 °C deformation) when the matrix was enriched with Nb solute atoms, the number densities of Nb and Nb-C clusters were high and this of the Nb-rich particles was low. These may indicate a stronger grain boundary pinning effect from the Nb atoms and Nb/Nb-C clusters in the < 5 nm size range, compared to the Nb-rich precipitates in the > 20 nm size range.

Table 2 Summary of the parameters for Nb-rich precipitates and Nb-containing clusters

Re-heating temperature [°C]		1100		1250	
Deformation temperature [°C]		1075	975	1075	975
Nb in the matrix [wt %]		0.002	0.005	0.016	0.015
Nb clusters	Maximum cluster size [number of atoms]	10	8	12	16
	Maximum Guinier radius [nm]	2.1	1.4	1.6	1.7
	Number density [$\times 10^5$ μm^{-3}]	1.60	2.15	3.19	3.74
Nb-C clusters	Maximum cluster size [number of atoms]	53	72	92	53
	Maximum Guinier radius [nm]	3.0	3.6	4.1	3.0
	Number density [$\times 10^5$ μm^{-3}]	0.20	2.0	4.3	7.0
Nb-rich particles	Average diameter (20-70 nm range) [nm]	26	22	29	29
	Number density (20-70 nm range) [μm^{-3}]	3.13	12.06	2.05	2.75
Austenite grain size [µm]		10	6	9	Partial recrystal.

Conclusion

In the studied NbTi-microalloyed steel the Nb solute atoms and Nb / Nb-C clusters in the < 5 nm size range were more effective in retarding recrystallisation than Nb-rich particles in the > 20 nm size range, due to a much higher number density of the clusters than that of the particles.

Acknowledgement: the authors are thankful to CBMM, BlueScope Steel Ltd., the ARC (LP110100231) for financial support of the project and to the AMMRF for technical support.

References

1. B. Dutta and C. M. Sellars, Materials Science and Technology, 3 (1987) 197-206.
2. S. Vervynckt, K. Verbeken, P. Thibaux, Y. Houbaert, Materials Science and Engineering A, 528 (2011) 5519 - 5528.
3. H.S. Zurob, G. Zhu, S.V. Subramanian, G.R. Purdy, C.R. Hutchinson and Y. Brechet, ISIJ Int., 45 (2005) 713 – 722.
4. C.R. Hutchinson, H.S. Zurob, C.W. Sinclair and Y.J.M. Brechet, Scripta Materialia, 59 (2008) 635 - 637.
5. C.L. Miao, C.J. Shang, H.S. Zurob, G.D. Zhang, and S.V. Subramanian, Metallurgical and Materials Transactions A, 43A (2012) 665 - 676.
6. A. J. DeArdo, International Materials Reviews, 48 (2003)371 - 402.
7. B. Dutta, E.J. Palmiere and C. M. Sellars, Acta Materialia 49 (2001) 785–794.
8. Y. Xu, Y. Yu, X. Liu and G. Wang, Journal of Material Science and Technology, 22 (2006) 149 – 152.
9. S. G. Hong, K.B. Kang and C.G. Park, Scripta Materialia, 46 (2002) 163 – 168.
10. S. Okaguchi and T. Hashimo, ISIJ International, 32 (1992) 283-290.
11. Y. Zeng and W. Wang, Journal of Material Science, 43 (2008) 874-882.
12. J.-S. Park, Y.-S. Ha, S.-J. Lee and Y.-K. Lee, Metallurgical and Materials Transactions A, 40A (2009) 560 – 568.
13. L. Yao, J.M. Cairney, C. Zhu and S.P. Ringer, Ultramicroscopy, 111 (2011) 648-651.
14. B.G. Gault, M.P. Moody, J.M. Cairney, S.P. Ringer, Atom probe microscopy, Springer, 2012.